

1 **Genetic engineering and molecular characterization of yeast strain expressing**
2 **hybrid human-yeast squalene synthase as a tool for anti-cholesterol drug**
3 **assessment**

4

5

6 Ilona Warchol¹, Monika Gora¹, Monika Wysocka-Kapcinska¹, Joanna Komaszyl¹,
7 Ewa Swiezewska¹, Maciej Sojka², Witold Danikiewicz², Danuta Plochocka¹, Agata
8 Maciejak¹, Dorota Tulacz¹, Agata Leszczynska¹, Suman Kapur³, Beata Burzynska^{1*}

9

10

11 ¹ Institute of Biochemistry and Biophysics, Polish Academy of Sciences, Warsaw,
12 Poland

13 ² Institute of Organic Chemistry, Polish Academy of Sciences, Warsaw, Poland

14 ³ Department of Biological Science, Birla Institute of Technology & Science (BITS),
15 Hyderabad, India

16

17 Running headline: Analysis of human-yeast SQS

18

19 * **Correspondence to:** Beata Burzynska,

20 Institute of Biochemistry and Biophysics, Polish Academy of Sciences,

21 Pawinskiego 5A, 02-106 Warsaw, Poland,

22 Phone number: +4822 5921214, Fax number: +4822 6584636,

23 Email: atka@ibb.waw.pl

24

25

26 **Abstract**

27

28 **Aims:** The main objective of the study is molecular and biological characterization of
29 the human-yeast hybrid squalene synthase, as a promising target for treatment of
30 hypercholesterolemia.

31 **Methods and Results:** The human-yeast hybrid squalene synthase, with 67% amino
32 acids, including the catalytic site derived from human enzyme, was expressed in *S.*
33 *cerevisiae* strain deleted of its own squalene synthase gene. The constructed strain has a
34 decreased level of sterols compared to the control strain. The mevalonate pathway and
35 sterol biosynthesis genes are induced and the level of triacylglycerols is increased.
36 Treatment of the strain with rosuvastatin or zaragozic acid, two mevalonate pathway
37 inhibitors, decreased the amounts of squalene, lanosterol and ergosterol, and up-
38 regulated expression of several genes encoding enzymes responsible for biosynthesis of
39 ergosterol precursors. Conversely, expression of the majority genes implicated in the
40 biosynthesis of other mevalonate pathway end-products, ubiquinone and dolichol, was
41 down-regulated.

42 **Conclusions:** The *S. cerevisiae* strain constructed in this study enables to investigate
43 the physiological and molecular effects of inhibitors on cell functioning.

44 **Significance and Impact of the Study:** The yeast strain expressing hybrid squalene
45 synthase with the catalytic core of human enzyme is a convenient tool for efficient
46 screening for novel inhibitors of cholesterol-lowering properties.

47

48 **Keywords:** mevalonate pathway, squalene synthase, sterol biosynthesis inhibitors,
49 yeast expression system, heterologous proteins

50

51 **Introduction**

52 Conversion of HMG-CoA to mevalonate is an early step in the cholesterol biosynthesis.
53 Mevalonate is also a precursor for biologically important nonsteroidal isoprenoids, for
54 example: dolichol, ubiquinone, isopentenyl tRNA and prenylated proteins, which have
55 an important role in the regulation of cellular processes. Statins, by competitive
56 inhibition of the HMG-Co reductase (HMGR) reduce endogenous cholesterol
57 production, increase the number of LDL receptors and thereby lower the serum
58 cholesterol level (Opie 2015). Although statin therapy is commonly assumed to be well
59 tolerated, serious adverse effects have been reported. Therefore, it is postulated that
60 some statins side effects may be due to the fact that statins suppress all post mevalonate
61 biosynthesis steps including non-steroidal isoprenoids (Charlton-Menys and Durrington
62 2008). Probably inhibition of HMGR, a key regulator of the mevalonic acid pathway,
63 causes not only decrease of cholesterol biosynthesis, but also disturbances in the
64 synthesis of other molecules like isopentyl diphosphate, farnesyl diphosphate and
65 geranylgeranyl diphosphate. Hence, there is a need for new medicines to lower
66 cholesterol levels, without any serious adverse reactions and also effective against
67 hypercholesterolemia (Seiki and Frishman 2009).

68 In both humans and yeast the mevalonate pathways are highly conserved (Fig.
69 1). They are identical till the zymosterol formation with the end product in human cells
70 being cholesterol, and ergosterol in yeast. The use of yeast as a host for the expression
71 of heterologous proteins has become increasingly popular in recent years (Nielsen
72 2009). As an eukaryote, *S. cerevisiae* has many of the advantages of higher eukaryotic
73 expression systems such as protein processing, protein folding and posttranslational
74 modifications, while being as easy to manipulate as the bacteria *E. coli*. As a model of

75 fundamental cellular processes and metabolic pathways of the human, yeast have
76 improved the understanding and facilitated the molecular analysis of many disease
77 genes (Menacho-Márquez and Murguía 2007; Ruggles *et al.* 2014). Comparative
78 genomics studies have shown that 40% of yeast proteins show homology to at least one
79 human protein and 30% of genes involved in human disease pathology have an ortholog
80 in yeast (Sturgeon 2006). Also, many regulatory pathways are conserved between yeast
81 and humans. Therefore, yeast emerge as an attractive model in drug development
82 studies like identification of new drug targets, target-based and non-target based drug
83 screening and analysis of the cellular effects of drugs (Hughes 2002; Wysocka-
84 Kapcinska *et al.* 2009; Marjanovic *et al.* 2010).

85 In our study, squalene synthase (SQS), the first dedicated enzyme of sterol
86 biosynthesis, has been chosen as a promising target for treatment of
87 hypercholesterolemia. Squalene synthase catalyzes the conversion of *trans*-farnesyl
88 diphosphate to squalene, the first specific step in the cholesterol biosynthetic pathway,
89 and is responsible for the flow of metabolites into either the sterol or the non sterol
90 branch of the pathway (Do *et al.* 2009). Squalene synthase inhibitors (SSIs) reduced
91 hepatic cholesterol biosynthesis by the induction of hepatic LDL receptors in a similar
92 way to statins (Charlton-Menys and Durrington 2007). Several classes of squalene
93 synthase inhibitors have been studied as potent inhibitors of squalene synthase
94 (Kourounakis 2011). For example, the fungal metabolite zaragozic acids or squalostatins
95 have been investigated as potent inhibitors of squalene synthase in human and other
96 species (Liu *et al.* 2012). SSIs do not cause myotoxicity, and when administered
97 together with a statin, reduce the statin-induced myotoxicity (Nishimoto *et al.* 2007).
98 On the other hand, most of SSIs failed to pass clinical phase I/II trials because of their

99 hepatotoxicity (Liao 2011). Nevertheless, squalene synthase is still considered as a
100 promising target for therapeutic molecules that could decrease cholesterol level without
101 affecting other isoprenoids.

102 Yeast and human squalene synthase amino acid sequences show 36% amino
103 acid identity and 57% similarity. Apart from the amino and carboxyl termini, which are
104 not similar, the conservation of sequences responsible for the catalytic activity of the
105 protein is very high (Robinson *et al.* 1993). The activity of squalene synthase is
106 essential for cell growth in yeast (Jennings *et al.* 1991), and a deletion of the *ERG9* gene
107 encoding yeast SQS is lethal. It has been shown previously that human FDFT1 gene
108 encoding hSQS expressed in yeast cells lacking native squalene synthase (*erg9Δ*) fails
109 to restore viability of the defective strain (Robinson *et al.* 1993; Soltis *et al.* 1995).

110 In this study, we present molecular and biological characterization of the human-
111 yeast hybrid squalene synthase, containing 67% of human SQS including the catalytic
112 site. Moreover, we analyse the impact of selected mevalonate pathway inhibitors on the
113 cell metabolism. Proposed by us, yeast model expressing hybrid squalene synthase with
114 the catalytic core of human SQS allows rapid, inexpensive, highly efficient screening of
115 *in silico* designed substances of cholesterol-lowering properties. Its application for such
116 screening will result in elimination of molecules of less effectiveness or causing adverse
117 effect.

118

119 **Materials and methods**

120

121 **Media and growth conditions**

122 *Saccharomyces cerevisiae* strains were cultivated in standard YP medium (1% Bacto-
123 yeast extract, 1% Bacto-peptone) containing 2% dextrose (YPD), 3% glycerol (YPGly),
124 or 3% ethanol (YPEtOH). Synthetic SD minimal medium (0.67% Bacto-yeast nitrogen
125 base, 2% dextrose) supplemented with a required synthetic complete amino acids drop-
126 out mixture (Sunrise Science Products, San Diego, CA, USA) was used for selection of
127 yeast cells bearing plasmids. Solid media were prepared by the addition of 2% Bacto-
128 agar. *URA3* counter-selection of yeast was carried out on SD plates supplemented with
129 0.1% 5-fluoroorotic acid (5-FOA; Sigma-Aldrich, St. Louis, MO, USA) and required
130 amino acids. To select cells containing the *kanMX4* cassette, YPD was supplemented
131 with geneticin (G418 sulphate, Sigma-Aldrich) at the concentration of 200 $\mu\text{g ml}^{-1}$. To
132 induce membrane permeability, nystatin (Sigma-Aldrich) was added to YPD to the final
133 concentration of 5 $\mu\text{g ml}^{-1}$. Rosuvastatin stock solution (10 mg ml^{-1}) was prepared by
134 extracting an active substance from Crestor (AstraZeneca AB, Sweden), as described
135 previously (Maciejak *et al.* 2013). Zaragozic acid (Sigma-Aldrich) was dissolved in
136 DMSO to obtain 10 mg ml^{-1} stock solution. Yeast cells were grown aerobically either in
137 liquid or on solid medium, at 28°C. To perform growth curves overnight cultures were
138 diluted to the concentration of 0.5×10^7 cells/ml and cells were grown in SD-HIS
139 medium at 28°C for 14 hours. Optical density (OD_{600}) measurements were done after
140 every two hours of cultivation. Each culture was assayed in triplicate and the results
141 were averaged.

142

143 **Homology modeling of human and yeast SQS structure**

144 Models of yeast and hybrid SQS fragments (34-383 and 35-376, respectively) were
145 obtained using SYBYLx2.1, TRIPOS Inc., on the basis of human SQS structure (PDB

146 entry 3VJ8) (Liu *et al.* 2012). The model structures were subjected to staged energy
147 minimization using AMBERFF99 forcefield, 100 steps. The model structure of
148 zaragozic acid complexed with hybrid SQS was obtained on the basis of the structure of
149 human SQS in complex with zaragozic acid (3VJC), (Liu *et al.* 2012).

150

151 **DNA manipulations and plasmid construction**

152 Standard protocols were used for all DNA manipulations (Green and Sambrook 2012).
153 The *Escherichia coli* strain XL1-Blue MRF' (Stratagene, La Jolla, CA, USA) was used
154 for cloning and propagation of plasmids. The sequences of all primers and methodology
155 of plasmid construction are shown in the Supporting Information, Table S1 and Figure
156 S1, respectively. The *ERG9* gene, encoding yeast SQS, was amplified with BamERG9
157 and ERG9SalI primers and ligated into pGEM-T Easy vector (Promega, Madison, WI,
158 USA). The FDFT1 cDNA, encoding human SQS, was amplified with 1FDFTbam and
159 2FDFTeco primers and ligated into pGEM-T Easy. The resulting plasmids served as
160 templates to construct hybrid squalene synthase (*HYB*). Both plasmids were digested
161 with MscI and SalI and the *ERG9* MscI-SalI fragment was subcloned into MscI-SalI cut
162 FDFT1/pGEM. Next, the resulting plasmid was digested with MscI and ligated with the
163 MscI-MscI fragment of FDFT1 gene to form *HYB*/pGEM. Tagging of *HYB* sequence
164 with *6HA* was carried out by PCR-amplification of *HYB* from *HYB*/pGEM using
165 HindHYB and HYBSalI primers and cloning into HindIII-SalI digested pYM16 (Janke
166 *et al.* 2004). Next, the promoter of *ERG9* gene, amplified with HinpERG9 and
167 pERG9Hin primers, was introduced into HindIII site of *HYBHA*/pYM16 plasmid.
168 Finally, P_{ERG9}-*HYBHA* was cloned into NotI and SmaI cut pRS313 (Sikorski and Hieter
169 1989). The analogous vector carrying *ERG9* tagged with *6HA* was constructed by PCR-

170 amplification of the P_{ERG9} -*ERG9HA* sequence with NotI $ERG9$ and $ERG9$ XmaI primers
171 from genomic DNA of the *ERG9HA* strain (construction details in the Supplementary
172 Material). The amplified P_{ERG9} -*ERG9HA* fragment was cloned into NotI-XmaI digested
173 pRS313.

174

175 **Construction of yeast strains expressing recombinant squalene synthase**

176 The *Saccharomyces cerevisiae* BY4741 and heterozygous diploid *erg9 Δ /ERG9* in the
177 background of BY4743 (EUROSCARF, Frankfurt, Germany) were used as the parental
178 strains for yeast strains constructed in this study. All yeast strains are listed in the
179 Supporting Information, Table S2. Yeast transformation was performed according to
180 Gietz and Woods (2002). Heterozygous diploid *erg9 Δ /ERG9* was transformed with
181 P_{GALI} -*ERG9*/pYES2 plasmid, sporulated and tetrads were dissected and cultured on
182 YPD plates. Haploid *erg9 Δ* [P_{GALI} -*ERG9*] was selected after replica plating on YPD
183 supplemented with geneticin and SD-URA. This haploid served for further
184 constructions of strains expressing yeast and hybrid squalene synthase. In order to
185 construct the *erg9 Δ* [P_{ERG9} -*HYBHA*] strain expressing human-yeast hybrid squalene
186 synthase, the P_{ERG9} -*HYBHA*/pRS313 plasmid was transformed into *erg9 Δ* [P_{GALI} -*ERG9*]
187 strain. Subsequently, the P_{GALI} -*ERG9*/pYES2 plasmid was lost on SD-HIS plates
188 containing 5-FOA to obtain the investigated strain. The *erg9 Δ* [P_{ERG9} -*ERG9HA*] control
189 strain was obtained by transformation of *erg9 Δ* [P_{GALI} -*ERG9*] strain with P_{ERG9} -
190 *ERG9HA*/pRS313. Next, the P_{GALI} -*ERG9*/pYES2 plasmid was lost on SD-HIS plates
191 containing 5-FOA.

192

193 **Lipid extraction**

194 Yeast strains were grown in SD-HIS medium with or without an inhibitor, starting from
195 0.5×10^7 cells/ml. After 10 hours, cells were spun down, pellets were weighed and lipid
196 extraction was performed according to the procedure described by Folch *et al.* (1957)
197 with minor changes, namely 16 μg cholestanol/sample was added as an internal
198 standard. Cells were homogenized with chloroform/methanol (1:1) and 0.063-0.200 mm
199 Silica Gel 60 (Merck, Darmstadt, Germany) by 5 min vortexing and overnight shaking.
200 Homogenates were spun down, solvent was removed to new tubes and remaining pellets
201 were re-extracted twice for 5 hours. Extracts were pooled and washed three times with
202 1/5 volume of 0.9% NaCl solution. The lower, chloroform phase containing lipids was
203 transferred to new tube and the solvent was evaporated under a stream of nitrogen and
204 dissolved in chloroform:methanol to yield crude lipid extract. For sterol analysis an
205 aliquot of crude lipid extract was dried and hydrolyzed after supplementation with
206 ethanol/toluene/water (82:100:15) solution with 7.5% KOH (w/v) for 2 hours at 100°C.
207 Lipids were extracted with equal volume of diethyl ether, the upper phase was
208 transferred to a new tube and the lower phase was re-extracted twice with diethyl ether,
209 then the extracts were pooled and evaporated and lipids were dissolved in 500 μl hexane.
210

211 **GC/MS analysis of lipids**

212 The Agilent 5975C GC/MSD (a gas chromatograph and a mass spectrometer detector of
213 Agilent Technologies, Santa Clara, CA) equipped with a 30 m long HP-5ms column,
214 with 0.25 mm inner diameter, and 0.25 μm stationary phase film thickness were used. 1
215 μl of lipid sample (hexane extract) was injected and the column temperature was set at
216 150°C for 5 min, next it was increased to 300°C with the ramp of 5°C/min and the final
217 temperature was set at 300°C for 30 min. Helium was used as a carrier gas and the flow

218 rate was set on 1 ml/min. The scan mode of 33-600 m/z was used to monitor mass
219 spectra. Sterols were identified by comparing their spectra with the those of the NIST
220 Mass Spectral Program (NIST/EPA/NIH Mass Spectral Library Version 2.0f). Area
221 under the signals of sterol and of internal control (cholestanol) served to calculate the
222 amount of sterol.

223

224 **TLC lipid analysis**

225 A thin layer chromatography (TLC) was carried out for crude lipid extract. Samples
226 were evaporated and dissolved in the appropriate amount of chloroform so that an equal
227 concentration of total lipids in each sample was achieved. 50 µl of each sample
228 corresponding to 60 µg of wet yeast mass spotted on a TLC plate (Silica Gel 60 F254
229 0.2 mm) and the plate was developed with petrol ether/diethyl ether/acetic acid
230 (90:10:1) as a mobile phase. Subsequently, the plate was dried and lipids were
231 visualized by iodine vapor. Densitometric analysis of freshly stained TLC
232 chromatogram, covered with a glass plate to avoid iodine desorption, was performed to
233 estimate the relative lipid content (ImageJ2x software, Java-based image processing
234 program, developed at the National Institutes of Health). Lipids were identified by
235 comparison with external standards.

236

237 **Quantitative real-time RT-PCR**

238 Yeast strains were grown in SD-HIS medium with or without an inhibitor, starting from
239 0.5×10^7 cells/ml. Each culture was prepared in three independent replicates. After 10
240 hours, cells were harvested, homogenized with MagNA Lyser Instrument (Roche
241 Diagnostics GmbH, Germany) and total RNA was isolated with MagNA Pure Compact

242 Instrument (Roche) according to the manufacturer's instruction. cDNA was synthesized
243 with QuantiTect Reverse Transcription Kit (Qiagen, Hilden, Germany), following the
244 instruction. Primers used for RT-qPCR are presented in the Supporting Information,
245 Table S3. RT-qPCR was carried out in 96-well plates using the LightCycler FastStart
246 DNA Master SYBR Green I and the LightCycler 480 System (Roche). Each sample was
247 run in triplicate. In order to calculate the relative expression ratio of genes between
248 experimental and control samples, the Pfaffl model (Pfaffl 2001) was used and
249 calculations were carried out in the REST-MCS v2 software tool. The expression data
250 were normalized to the reference gene *ACT1*. All experiments were performed
251 according to the MIQE guidelines (Bustin *et al.* 2009).

252

253 **Results**

254

255 **Human and yeast SQS models show different structures**

256 A comparison of the modeled yeast SQS structure with that of the experimentally
257 derived human SQS structure of the human and yeast SQS proteins showed no major
258 differences around the active center, but significant structural alterations between the
259 yeast fragments N113-D119 and D161-T171, and the corresponding human SQS
260 regions M112-D118 and D159-S164 (Supporting Information, Fig. S2). These
261 fragments are located in close proximity to the central cavity, so one may expect
262 differences in the binding of inhibitors to the human and yeast squalene synthases.
263 Taking into consideration all the above-mentioned aspects, a hybrid squalene synthase
264 with the catalytic core of human SQS was constructed in this study. A model structure
265 of the hybrid SQS was compared with the structure of human SQS. On the basis of

266 published data (Liu *et al.* 2012; Liu *et al.* 2014; Shang *et al.* 2014) it was established
267 that residues constituting the active center of human SQS are located in fragment 35 -
268 327 of the enzyme. Superposition of backbone atoms of the 35 -327 fragment gave an
269 RMSD (root mean square deviation) of about 0.1 Å between the human and the hybrid
270 enzyme, what means that both structures are virtually identical in that region.
271 Differences between both structures appear at the C-terminal part of the protein, which
272 is far away from the active site. Fig. 2 presents a comparison of the main chain course
273 of the human and the hybrid SQS. The part of human SQS structure (P354 - K358)
274 substantially different from the hybrid SQS is also shown.

275

276 ***HYBHA* hybrid gene restores *erg9Δ* viability**

277 *S. cerevisiae erg9Δ* strain bearing the FDFT1-*ERG9* hybrid gene (*HYBHA*) was
278 constructed similar to Robinson *et al.* (1993). The hybrid squalene synthase comprised
279 67% of human SQS aa sequence (1-296 amino acids) including the catalytic site, and
280 33% of yeast SQS sequence (304-444 amino acids), which included transmembrane
281 domain necessary for the attachment of protein to the membranes of endoplasmic
282 reticulum (Supporting Information, Fig. S3). Importantly, in our study the squalene
283 synthase hybrid gene was expressed from the native *ERG9* promoter, and was fused on
284 its 3' end with hemagglutinin (*HA*) tag sequence. The P_{*ERG9*}-*HYBHA* construct was
285 cloned into centromeric pRS313 vector and was expressed in yeast *erg9Δ* strain.
286 Control strains *erg9Δ* bearing P_{*ERG9*}-*ERG9HA* on pRS313 and BY4741 transformed
287 with an empty pRS313 vector were also constructed.

288 On the contrary to the full-length human FDFT1 gene, the human-yeast hybrid
289 gene *HYBHA* was able to restore viability of *erg9Δ* yeast cells. All tested strains were

290 growing equally on a complete medium, a minimal (histidine lacking) medium and
291 glycerol or ethanol containing medium at 28°C (Fig. 3a). No statistically significant
292 difference between the growth curves was observed (Fig. 3b).

293 Additionally, all strains were tested on nystatin supplemented medium (Fig. 3c).
294 Nystatin is a polyene macrolide antibiotic which forms ion channels on plasma
295 membrane, resulting in cation leakage and cell death. The nystatin activity was shown
296 to be significantly affected by the ergosterol membrane's molar fraction (Kristanc *et al.*
297 2014). The *HYBHA* expressing strain was resistant to nystatin, which might be due to
298 lowered content of ergosterol in plasma membranes.

299

300 **Sterol biosynthesis is disturbed in *HYBHA* expressing strain**

301 To evaluate the level of squalene and sterol in yeast cells, gas chromatography/mass
302 spectrometry (GC/MS) analysis of lipids was performed. The content of squalene,
303 lanosterol and ergosterol was diminished in *HYBHA* expressing strain, and it reached
304 the level of 10.9% (p=0.035), 43.7% (p=0.094) and 82.3% (p=0.342) respectively, in
305 comparison to the control strain (Fig. 4a).

306 Since the sterol biosynthesis was impaired in the *erg9Δ* [*P_{ERG9}-HYBHA*] strain,
307 sterol storage forms might be modified as a result of diminished sterol content. Sterols
308 are stored in yeast cells in the form of esters and they are located in lipid particles (LP)
309 together with triacylglycerols (Czabany *et al.* 2007). As tested by semiquantitative thin
310 layer chromatography method (TLC), the *erg9Δ* [*P_{ERG9}-HYBHA*] strain showed a
311 different profile of lipids than the control (Fig. 4b). Both, the level of free ergosterol and
312 also ergosterylesters was reduced. On the contrary, the level of triacylglycerols and free
313 fatty acids was increased.

314 **mRNA expression level of isoprenoid biosynthesis pathway genes is changed in**
315 ***HYBHA* expressing strain**

316 Quantification of mRNA for genes encoding selected enzymes (shown in Fig. 1) from
317 the sterol and non-sterol isoprenoid biosynthesis pathways was performed by RT-qPCR.
318 Gene expression levels in the *erg9Δ* [*P_{ERG9}-HYBHA*] strain cultured at 28°C were
319 related to the expression of respective genes in *erg9Δ* [*P_{ERG9}-ERG9HA*] strain grown at
320 the same temperature (Fig. 5a and b). The expression of all the tested genes of sterol
321 biosynthesis was induced (Fig. 5a), except for the *HMG2* gene which is one of the yeast
322 paralogues coding for HMG-CoA reductase. The expression of genes coding for
323 enzymes of other mevalonate-end products was only slightly changed in the *erg9Δ*
324 [*P_{ERG9}-HYBHA*] strain (Fig. 5b), the majority of them were down-regulated.

325

326 **The levels of squalene and sterols are lowered in *HYBHA* expressing strain**
327 **cultured with inhibitors**

328 The constructed *erg9Δ* [*P_{ERG9}-HYBHA*] strain was used in further tests of two inhibitors
329 of the mevalonate pathway: zaragozic acid – inhibitor of squalene synthase, and
330 rosuvastatin – inhibitor of HMG-CoA reductase. They were chosen to compare the
331 effect of the inhibition of the mevalonate pathway at the level of SQS and HMGR. To
332 this end, median lethal dose of inhibitors (LD₅₀) was assessed at permissive temperature
333 of 28°C. The final concentration of 1.3 μmol l⁻¹ for zaragozic acid and 22.8 μmol l⁻¹ for
334 rosuvastatin were needed for 50% growth inhibition after 10 hours of cultivation.

335 To determine the influence of zaragozic acid and rosuvastatin on squalene and
336 sterol content in *HYBHA* expressing strain, GC-MS analysis was performed for lipids
337 isolated from cells grown in the presence or absence of the respective inhibitor. As

338 expected, both inhibitors decreased the levels of squalene, lanosterol and ergosterol.
339 The effect of rosuvastatin on sterol biosynthesis inhibition was higher than that of
340 zaragozic acid at the same toxic dose of LD₅₀. The amount of lipids was reduced to:
341 4.6% vs 17.5% (p=0.032) for squalene, 4.3% vs 21.6% (p=0.005) for lanosterol and
342 60% vs 80.8% (p=0.093) for ergosterol, by rosuvastatin and zaragozic acid, respectively
343 (Fig. 6).

344

345 **Inhibition of the mevalonate pathway alters the expression of selected genes**

346 Rosuvastatin and zaragozic acid act at different points of the mevalonate pathway,
347 might differently affect the availability of FPP. Rosuvastatin, by inhibition of the early
348 step of the pathway, diminishes the cellular level of farnesyl diphosphate (Liao 2002).
349 On the contrary, blocking the major FPP utilizing branch at the level of squalene
350 synthase results in elevated FPP availability. Taking this into account, the expression of
351 mevalonate pathway genes, especially genes from side branches in response to inhibitor,
352 was followed. RT-qPCR analysis was performed for the *erg9Δ* [*P_{ERG9}-HYBHA*] strain
353 cultured with or without the respective inhibitor.

354 As was expected, genes of the early mevalonate pathway and sterol biosynthesis
355 branch were up-regulated in response to both inhibitors (Fig. 7a, left diagram). On the
356 contrary, the expression of genes of other isoprenoid pathway-end products, below the
357 FPP-branching was mostly decreased, except for *MOD5* (Fig. 7a, right diagram).
358 Surprisingly, the tendency of changes in mRNA levels was consistent for both
359 inhibitors. In order to check whether increased doses of inhibitors would enhance the
360 changes in gene expression, RT-qPCR was performed for the *HYBHA* expressing strain
361 inhibited with LD₇₀ dose of rosuvastatin or zaragozic acid. Indeed, although the general

362 trend seemed similar, the rate of up- or down-regulation was better pronounced (Fig.
363 7b) than in case of LD₅₀.

364 The mRNA level of hybrid squalene synthase was up-regulated in response to
365 treatment with inhibitors (Fig. 7a and b). Also the level of SQS protein was slightly
366 increased by both rosuvastatin and zaragozic acid (Supporting Information, Fig. S4).

367

368 **Discussion**

369 Since a comparison of modeled structures of yeast and human squalene synthases
370 revealed substantial conformational differences close to the central cavity, a hybrid SQS
371 was constructed. The human-yeast hybrid squalene synthase, containing 67% of human
372 SQS aa, including the catalytic site, was expressed in *Saccharomyces cerevisiae erg9Δ*
373 strain in order to define the utility of yeast as a tool for screening human SQS inhibitors.
374 The *ERG9* gene expression in yeast has been reported to undergo complex regulation,
375 both positive and negative, by diverse factors through *cis*-elements in the promoter
376 (Kennedy *et al.* 1999; Kennedy and Bard 2001). Using the native *ERG9* promoter to
377 drive expression of the hybrid SQS gene we ensured its proper regulation and
378 expression. This is crucial because squalene synthase constitutes an important point of
379 the mevalonate pathway, second to HMG-CoA reductase, that is regulated by a sterol
380 feedback mechanism and is responsible for directing substrates to different branches of
381 the pathway.

382 Although during standard growth conditions the *erg9Δ* [*P_{ERG9}-HYBHA*] strain
383 behaves like a control strain, it is resistant to nystatin. Nystatin was previously reported
384 to be specific for ergosterol in yeast cell membranes (Walker-Caprioglio 1989), and
385 sterol mutants (e.g. *ERG7*, *ERG6*, *ERG5*) are resistant to nystatin (SGD Database,

386 <http://www.yeastgenome.org>). This might suggest that qualitative or quantitative
387 changes in sterol content of yeast cellular membranes are correlated with resistance to
388 nystatin. GC-MS analysis, indeed, showed that the strain expressing hybrid SQS has
389 diminished amount of squalene, lanosterol and ergosterol.

390 Mevalonate pathway regulation is very complex and only partially understood,
391 however, it is known to proceed at multiple levels, such as transcriptional activation and
392 repression, maintaining protein stability or stimulating protein degradation, and it
393 involves sterol and non-sterol intermediates of the pathway. In general, genes of the
394 early part of mevalonate pathway as well as genes of sterol biosynthesis branch are
395 overexpressed in the *HYBHA* expressing strain, except the *MG2* gene, which is slightly
396 down-regulated. We suspect that the overexpression is caused by a sterol-mediated
397 feedback response, which has previously been reported both in mammalian and yeast
398 cells (Dimster-Denk *et al.* 1994; Dimster-Denk *et al.* 1999).

399 The second important regulation point of the mevalonate pathway resides at the
400 level of FPP, which is considered as the common precursor for numerous isoprenoids.
401 The expression of genes placed in the intersectional pathways (shown in Fig. 1) is
402 generally decreased in the *erg9Δ* [*P_{ERG9}-HYBHA*] strain. Perhaps the underlying reason
403 is an effort of cells to redirect the flux of FPP to the impaired sterol biosynthetic
404 pathway or a rescue mechanism in response to possibly increased level of farnesyl
405 diphosphate.

406 In summary, the yeast strain expressing the hybrid SQS contains a lower level of
407 sterols than the control strain although the amount of sterols is sufficient to maintain
408 normal growth at standard growth conditions. The diminished level of sterols triggers

409 an adaptive response of the cell, which includes an overexpression of the mevalonate
410 pathway and sterol biosynthesis branch genes.

411 We tested two inhibitors acting at different enzymes of the mevalonate pathway,
412 namely rosuvastatin and zaragozic acid that inhibit HMG-CoA reductase and squalene
413 synthase, respectively. A rationale for this selection was a possible contrapositive effect
414 on the pool of farnesyl diphosphate exerted by HMG-CoA and SQS inhibitors.

415 Inhibition of mevalonate pathway either at the level of HMGR or SQS affects
416 the synthesis of squalene and finally sterol production in the *erg9Δ* [*P_{ERG9}-HYBHA*]
417 strain. The most significant reduction was seen for ergosterol biosynthetic precursors,
418 such as squalene and lanosterol. On the contrary, the last product of the branch,
419 ergosterol, was only slightly decreased, which might be caused by efficient conversion
420 of precursors and mobilisation of sterol stored in lipid particles. Rosuvastatin appears to
421 impair sterol biosynthesis to a greater extent than zaragozic acid when compared at
422 LD₅₀. Sensitivity of the *erg9Δ* [*P_{ERG9}-HYBHA*] strain to mevalonate pathway inhibitors
423 proves that this strain may be successfully used for SQS inhibitor screening.

424 Rosuvastatin and zaragozic acid induced the expression of genes of the early
425 steps of mevalonate pathway (except the *HMG2* gene) and genes specific for sterol
426 synthesis. The enhanced expression was most likely related to the feedback response
427 triggered by decreased amounts of sterol. A similar effect on the expression of genes
428 along the mevalonate pathway in yeast observed during HMG-CoA and SQS inhibition
429 was reported by Dimster-Denk *et al.* (1999) and Kuranda *et al.* (2010). Due to an
430 opposite effect of the inhibition of HMGR and SQS, expected on FFP level, we
431 followed the mRNA levels of genes from the branching pathways for rosuvastatin and
432 zaragozic acid blocks. Inhibition of HMGR leads to a decreased amount of mevalonic

433 acid and depletion of downstream products along with farnesyl diphosphate (Liao
434 2002), which becomes less available for enzymes utilizing FPP. On the contrary, the
435 SQS block results in an elevated FPP level (Bergstrom *et al.* 1993), that may be more
436 accessible for FPP-consuming enzymes. We observed negligible effect of the inhibition
437 on *BTS1* and *RER2* expression, but the levels of *RAM1*, *COQ1* and *COX10* mRNA were
438 diminished in both tested strains. However, the directions of expression changes for
439 specific genes were consistent for both inhibitors, which is most likely related to the
440 influence of deficient sterols. Also the expression of other genes in branching pathways
441 was repressed, such as ubiquinone biosynthesis genes (*COQ3*, *CAT5*), dolichyl
442 phosphate biosynthesis gene (*SEC59*) and the gene coding for a protein that undergoes
443 farnesylation, *RAS1*. The only genes that were up-regulated were *COQ2* and *MOD5*, of
444 which the first is involved in ubiquinone biosynthesis and the second is responsible for
445 tRNA prenylation process. The alterations in the expression levels were even higher
446 when the growth of *HYBHA* bearing strain was inhibited by 70% what indicates that the
447 constructed strain demonstrates a dose – response effect.

448 *Saccharomyces cerevisiae* model that has been engineered in this study is a
449 convenient tool for high-throughput screening for molecules designed to inhibit the
450 catalytic site of human SQS. Moreover, the yeast model allows to study the
451 physiological and molecular effects of tested molecules on the cell, such as mRNA and
452 protein expression levels and lipid profile.

453

454 **Acknowledgements:** This work was supported by The National Science Centre, Poland
455 (N N302 634138).

456 **Conflict of Interest:** No conflict of interest declared.

457 **References**

- 458 Bergstrom, J.D., Kurtz, M.M., Rew, D.J., Amend, A.M., Karkas, J.D., Bostedor, R.G.,
459 Bansa, V.S., Dufresne, C., VanMiddlesworth, F.L., Hensens, O.D., Liesch, J.M.,
460 Zink, D.L., Wilson, K.E., Onishi, J., Milligan, J.A., Bill, G., Kaplan, L., Nallin
461 Omstead, M., Jenkins, R.G., Huang, L., Mein, M.S., Quinn, L., Burg, R.W.,
462 Kong, Y.L., Mochales, S., Mojena, M., Martin, I., Pelaez, F., Diez, M.T. and
463 Alberts, W. (1993) Zaragozic acids: a family of fungal metabolites that are
464 picomolar competitive inhibitors of squalene synthase. *Proc Natl Acad Sci USA*
465 **90**, 80-84.
- 466 Bustin, S.A., Benes, V., Garson, J.A., Hellemans, J., Huggett, J., Kubista, M., Mueller,
467 R., Nolan, T., Pfaffl, M.W., Shipley, G.L., Vandesompele, J. and Wittwer, C.T.
468 (2009) The MIQE guidelines: minimum information for publication of
469 quantitative real-time PCR experiments. *Clin Chem* **55**, 611-622.
- 470 Charlton-Menys, V. and Durrington, P.N. (2007) Squalene synthase inhibitors: clinical
471 pharmacology and cholesterol-lowering potential. *Drugs* **67**, 11-16.
- 472 Charlton-Menys, V. and Durrington P.N. (2008) Human cholesterol metabolism and
473 therapeutic molecules. *Exp Physiol* **93**, 27-42.
- 474 Czabany, T., Athenstaedt, K. and Daum, G. (2007) Synthesis, storage and degradation
475 of neutral lipids in yeast. *Biochim Biophys Acta* **1771**, 299-309.
- 476 Dimster-Denk, D., Rine, J., Phillips, J., Scherer, S., Cundiff, P., DeBord, K., Gilliland,
477 D., Hickman, S., Jarvis, A., Tong, L. and Ashby, M. (1999) Comprehensive
478 evaluation of isoprenoid biosynthesis regulation in *Saccharomyces cerevisiae*
479 utilizing the Genome Reporter Matrix. *J Lipid Res* **40**, 850-860.
- 480 Dimster-Denk, D., Thorsness, M.K. and Rine, J. (1994) Feedback regulation of 3-
481 hydroxy-3-methylglutaryl coenzyme A reductase in *Saccharomyces cerevisiae*.
482 *Mol Biol Cell* **5**, 655-665.
- 483 Do, R., Kiss, R.S., Gaudet, D. and Engert, J.C. (2009) Squalene synthase: a critical
484 enzyme in the cholesterol biosynthesis pathway. *Clin Genet* **75**, 19-29.
- 485 Folch, J., Lees, M. and Sloane-Stanley, G.H. (1957) A simple method for the isolation
486 and purification of total lipides from animal tissues. *J Biol Chem* **226**, 497-509.
- 487 Gietz, R. and Woods, R. (2002) Transformation of yeast by the LiAc/SS carrier
488 DNA/PEG method. *Meth Enzymol* **350**, 87-96.

489 Green, M.R. and Sambrook, J. (2012) *Molecular Cloning: A Laboratory Manual*, fourth
490 ed. Cold Spring Harbor Laboratory Press, Cold Spring Harbor, N.Y.

491 Hughes, T.R. (2002) Yeast and drug discovery. *Funct Integr Genomics* **2**, 199-211.

492 Janke, C., Magiera, M.M., Rathfelder, N., Taxis, C., Reber, S., Maekawa, H., Moreno-
493 Borchart, A., Doenges, G., Schwob, E., Schiebel, E. and Knop, M. (2004) A
494 versatile toolbox for PCR-based tagging of yeast genes: new fluorescent proteins,
495 more markers and promoter substitution cassettes. *Yeast* **21**, 947-962.

496 Jennings, S.M., Tsay, Y.H., Fisch, T.M. and Robinson, G.W. (1991) Molecular cloning
497 and characterization of the yeast gene for squalene synthetase. *Proc Natl Acad Sci*
498 *USA* **88**, 6038-6042.

499 Kennedy, M.A., Barbuch, R. and Bard, M. (1999) Transcriptional regulation of the
500 squalene synthase gene (ERG9) in the yeast *Saccharomyces cerevisiae*. *Biochim*
501 *Biophys Acta* **1445**, 110-22.

502 Kennedy, M.A. and Bard, M. (2001) Positive and negative regulation of squalene
503 synthase (ERG9), an ergosterol biosynthetic gene, in *Saccharomyces cerevisiae*.
504 *Biochim Biophys Acta* **1517**, 177-189.

505 Kourounakis, A.P., Katselou, M.G., Matralis, A.N., Ladopoulou, E.M. and Bavavea, E.
506 (2011) Squalene synthase inhibitors: An update on the search for new
507 antihyperlipidemic and antiatherosclerotic agents. *Curr Med Chem* **18**, 4418-
508 4439.

509 Kristanc, L., Božič, B. and Gomišček, G. (2014) The role of sterols in the lipid vesicle
510 response induced by the pore-forming agent nystatin. *Biochim Biophys Acta* **1838**,
511 2635-2645.

512 Kuranda, K., François, J. and Palamarczyk, G. (2010) The isoprenoid pathway and
513 transcriptional response to its inhibitors in the yeast *Saccharomyces cerevisiae*.
514 *FEMS Yeast Res* **10**, 14-27.

515 Liao, J.K. (2002) Isoprenoids as mediators of the biological effects of statins. *J Clin*
516 *Invest* **110**, 285-288.

517 Liao, J.K. (2011) Squalene synthase inhibitor lapaquistat acetate: could anything be
518 better than statins? *Circulation* **123**, 1925-1928.

519 Liu, C.I., Jeng, W.Y., Chang, W.J., Ko, T.P. and Wang, A.H. (2012) Binding modes of
520 zaragozic acid A to human squalene synthase and staphylococcal
521 dehydrosqualene synthase. *J Biol Chem* **287**, 18750-18757.

522 Liu C.I, Jeng W.Y., Chang, W.J., Shih, M.F., Ko, T.P. and Wang, A.H.J. (2014)
523 Structural insights into the catalytic mechanism of human squalene synthase. *Acta*
524 *Crystallogr* **70**, 231-241.

525 Maciejak, A., Leszczynska, A., Warchol, I., Gora, M., Kaminska, J., Plochocka, D.,
526 Wysocka-Kapcinska, M., Tulacz, D., Siedlecka, J., Swiezewska, E., Sojka, M.,
527 Danikiewicz, W., Odolczyk, N., Szkopinska, A., Sygitowicz, G. and Burzynska,
528 B (2013) The effects of statins on the mevalonic acid pathway in recombinant
529 yeast strains expressing human HMG-CoA reductase. *BMC Biotechnol* **13**, 68.

530 Marjanovic, J., Chalupska, D., Patenode, C., Coster, A., Arnold, E., Ye, A., Anesi, G.,
531 Lu, Y., Okun, I., Tkachenko, S., Haselkorn, R. and Gornicki, P. (2010)
532 Recombinant yeast screen for new inhibitors of human acetyl-CoA carboxylase 2
533 identifies potential drugs to treat obesity. *Proc Natl Acad Sci USA* **107**, 9093-
534 9098.

535 Menacho-Márquez, M. and Murguía, J.R. (2007) Yeast on drugs: *Saccharomyces*
536 *cerevisiae* as a tool for anticancer drug research. *Clin Transl Oncol* **9**, 221-228.

537 Nielsen, J. (2009) Systems biology of lipid metabolism: from yeast to human. *FEBS*
538 *Lett* **583**, 3905-3913.

539 Nishimoto, T., Ishikawa, E., Anayama, H., Hamajyo, H., Nagai, H., Hirakata, M. and
540 Tozawa, R. (2007) Protective effects of a squalene synthase inhibitor, lapaquistat
541 acetate (TAK-475), on statin-induced myotoxicity in guinea pigs. *Toxicol Appl*
542 *Pharmacol* **223**, 39-45.

543 Opie, L.H. (2015) Present status of statin therapy. *Trends Cardiovasc Med* **25**, 216-225.

544 Pfaffl, M. (2001) A new mathematical model for relative quantification in real-time
545 RT-PCR. *Nucleic Acids Res* **29**, e45.

546 Robinson, G.W., Tsay, Y.H., Kienzle, B.K., Smith-Monroy, C.A. and Bishop, R.W.
547 (1993) Conservation between human and fungal squalene synthetases: similarities
548 in structure, function, and regulation. *Mol Cell Biol* **13**, 2706-2717.

549 Ruggles, K.V., Garbarino, J., Liu, Y., Moon, J., Schneider, K., Henneberry, A.,
550 Billheimer, J., Millar, J.S., Marchadier, D., Valasek, M.A., Joblin-Mills, A.,

551 Gulati, S., Munkacsi, A.B., Repa, J.J., Rader, D. and Sturley, S.L. (2014) A
552 functional, genome-wide evaluation of liposensitive yeast identifies the "ARE2
553 required for viability" (ARV1) gene product as a major component of eukaryotic
554 fatty acid resistance. *J Biol Chem* **289**, 4417-4431.

555 Seiki, S. and Frishman, W.H. (2009) Pharmacologic inhibition of squalene synthase and
556 other downstream enzymes of the cholesterol synthesis pathway: a new
557 therapeutic approach to treatment of hypercholesterolemia. *Cardiol Rev* **17**, 70-76.

558 Shang, N., Li, Q., Ko, T.P., Chan, H.C., Li, J., Zheng, Y., Huang, C.H., Ren, F., Chen,
559 C.C., Zhu, Z., Galizzi, M., Li, Z.H., Rodrigues-Poveda, C.A., Gonzalez-
560 Pacanowska, D., Veiga-Santos, P., de Carvalho, T.M., de Souza, W., Urbina, J.A.,
561 Wang, A.H., Docampo, R., Li, K., Liu, Y.L., Oldfield, E. and Guo, R.T. (2014)
562 Squalene synthase as a target for Chagas disease therapeutics. *PLoS Pathog* **10**,
563 e1004114.

564 Sikorski, R. and Hieter, P. (1989) A system of shuttle vectors and yeast host strains
565 designed for efficient manipulation of DNA in *Saccharomyces cerevisiae*.
566 *Genetics* **122**, 19-27.

567 Soltis, D.A., McMahon, G., Caplan, S.L., Dudas, D.A., Chamberlin, H.A, Vattay, A.,
568 Dottavio, D., Rucker, M.L., Engstrom, R.G., Cornell-Kennon, S.A. and Boettcher,
569 B.R. (1995) Expression, purification, and characterization of the human squalene
570 synthase: use of yeast and baculoviral systems. *Arch Biochem Biophys* **316**, 713-
571 723.

572 Sturgeon, C.M., Kemmer, D., Anderson, H.J. and Roberge, M. (2006) Yeast as a tool to
573 uncover the cellular targets of drugs. *Biotechnol J* **1**, 289-298.

574 Walker-Caprioglio, H.M., MacKenzie, J.M. and Parks, L.W. (1989) Antibodies to
575 nystatin demonstrate polyene sterol specificity and allow immunolabeling of
576 sterols in *Saccharomyces cerevisiae*. *Antimicrob Agents Chemother* **33**, 2092-
577 2095.

578 Wysocka-Kapcinska, M., Lutyk-Nadolska, J., Kiliszek, M., Plochocka, D., Maciag, M.,
579 Leszczynska, A., Rytka, J. and Burzynska, B. (2009) Functional expression of
580 human HMG-CoA reductase in *Saccharomyces cerevisiae*: a system to analyse
581 normal and mutated versions of the enzyme in the context of statin treatment. *J*
582 *Appl Microbiol* **106**, 895-902.

583

584 **Figure legends**

585

586 **Figure 1** The biosynthesis of ergosterol (yeast) and cholesterol (human). The enzymes
587 selected for gene expression analysis are shown at the corresponding steps of the
588 pathway. *ARE1* – sterol O-acyltransferase 1, *ARE2* – sterol O-acyltransferase 2, *BTS1* –
589 geranylgeranyl diphosphate synthase, *CAT5* – ubiquinone biosynthesis monooxygenase,
590 *COQ1* – hexaprenyl diphosphate synthase, *COQ2* – *para*-hydroxybenzoate-polyprenyl
591 transferase, *COQ3* – 3,4-dihydroxy-5-hexaprenylbenzoatemethyltransferase, *COX10* –
592 protoheme IX farnesyltransferase, *ERG1* – squalene monooxygenase, *ERG10* – acetyl-
593 CoA acetyltransferase, *ERG20* – farnesyl diphosphate synthase, *ERG3* – C-5 sterol
594 desaturase, *ERG6* – delta(24)-sterol C-methyltransferase, *ERG9* – squalene synthase,
595 *FDT1* – squalene synthase (human), *HMG1* – 3-hydroxy-3-methylglutaryl-Co A
596 reductase 1, *HMG2* – 3-hydroxy-3-methylglutaryl-Co A reductase 2, *MOD5* – tRNA
597 dimethylallyltransferase, *RAM1* – protein farnesyltransferase subunit beta, *RAM2* –
598 protein farnesyltransferase/geranylgeranyltransferase type-1 subunit alpha, *RER2* – *cis*-
599 prenyltransferase, *SEC59* – dolichol kinase. ZA – zaragozic acid.

600

601 **Figure 2** Structural comparison of human and hybrid SQS. Human protein is in green,
602 hybrid in blue (light blue for human part, dark blue for yeast part). Active center is
603 highlighted in yellow. Zaragozic acid is presented as sticks. Arrows indicate main
604 differences between human and hybrid SQS structures.

605

606 **Figure 3** The *HYBHA* hybrid gene complements the *ERG9* gene. (a) Serial dilutions of
607 the BY4741 strain bearing the empty vector, and both *ERG9HA* and *HYBHA* expressing

608 strains were spotted on YPD, minimal, glycerol and ethanol medium. Strains were
609 grown at 28°C. (b) The growth curve of *ERG9HA* and *HYBHA* expressing strains grown
610 in minimal liquid medium (without histidine) for 14 hours at 28°C. (■) *erg9Δ* [*P_{ERG9}-*
611 *ERG9HA*] and (○) *erg9Δ* [*P_{ERG9}-HYBHA*]. (c) The *HYBHA* expressing strain is resistant
612 to nystatin. Serial dilutions of the tested strains were spotted on YPD and YPD
613 supplemented with nystatin. Strains were grown at 28°C.

614

615 **Figure 4** Analysis of lipids. (a) The content of squalene and sterols in the *HYBHA* strain
616 is diminished in comparison to the control strain. Strains were cultured in minimal
617 (histidine lacking) medium at 28°C for 10 hours and lipid content was analyzed by
618 GC/MS. (□) *erg9Δ* [*P_{ERG9}-ERG9HA*]; (■) *erg9Δ* [*P_{ERG9}-HYBHA*] and (*) $p \leq 0.05$. (b)
619 The lipid profile is changed in the *HYBHA* strain comparing to the control strain. Strains
620 were cultured at 28°C for 10 hours, lipids were extracted and separated on TLC plates.
621 Numbers represent the ratio of the lipid in *HYBHA* expressing strain with respect to the
622 control strain. One representative analysis of three independent TLC experiments is
623 shown. (E) *erg9Δ* [*P_{ERG9}-ERG9HA*]; (H) *erg9Δ* [*P_{ERG9}-HYBHA*]; (SQ) squalene; (SE)
624 sterol esters; (TAG) triacylglycerols; (FFA) free fatty acids and (ERG) ergosterol.

625

626 **Figure 5** mRNA levels of selected genes encoding enzymes of sterol and nonsterol
627 biosynthesis pathways. (a) and (b) The expression of genes in the *erg9Δ* [*P_{ERG9}-*
628 *HYBHA*] strain relative to the expression in the control strain cultured at 28°C. mRNA
629 levels of genes coding for enzymes of the mevalonate pathway (1) above FPP and (2)
630 sterol biosynthesis are indicated on the right panel. mRNA levels of genes coding for
631 enzymes that participate in (3) protein prenylation, (4) ubiquinone biosynthesis, (5)

632 dolichol biosynthesis, (6) heme A biosynthesis, and (7) tRNA prenylation are indicated
633 on the left panel. Expression data were normalized to *ACT1* gene. Results are shown as
634 a \log_2 of relative expression. (*) $p \leq 0.05$ and (**) $p \leq 0.001$.

635

636 **Figure 6** The reduction of squalene and sterol content in *HYBHA* expressing strain is
637 dependent on the type of inhibitor used. The *erg9Δ* [*P_{ERG9}-HYBHA*] strain was cultured
638 in minimal (histidine lacking) medium at 28°C for 10 hours with (□) rosuvastatin or (■)
639 zaragozic acid. % of sterol concentration in comparison to the “no treatment” group.

640

641 **Figure 7** The expression of genes in the *erg9Δ* [*P_{ERG9}-HYBHA*] strain exposed to the
642 inhibitor relative to the expression in unexposed cells. Yeast cells were cultured at 28°C
643 for 10 hours in the presence or absence of the respective inhibitor at the dose of (a) LD₅₀
644 or (b) LD₇₀. mRNA levels of genes coding for enzymes of the mevalonate pathway (1)
645 above FPP and (2) sterol biosynthesis branch are indicated on the right panel. mRNA
646 levels of genes coding for enzymes that participate in (3) protein prenylation, (4)
647 ubiquinone biosynthesis, (5) dolichol biosynthesis, (6) heme A biosynthesis, and (7)
648 tRNA prenylation are indicated on the left panel. Expression data were normalized to
649 *ACT1* gene. Results are shown as a \log_2 of relative expression. (□) rosuvastatin; (■)
650 zaragozic acid; (*) $p \leq 0.05$ and (**) $p \leq 0.001$.

651

652 **Supporting Information**

653

654 **Table S1** Primers used for plasmid construction

655 **Table S2** Yeast strains used in this study

656 **Table S3** Sequences of primers used in real-time PCR

657 **Supporting Materials and methods:** Construction of the *ERG9HA* strain

658 **Supporting Materials and methods:** Immunodetection of HA-tagged squalene
659 synthase

660 **Figure S1** The methodology of plasmid construction. (a) Construction of hybrid
661 squalene synthase coding sequence (*HYB*). (b) Construction of $P_{ERG9-yHYBHA}/pRS313$
662 plasmid.

663 **Figure S2** Human SQS ribbon model. DXXED conserved motifs are highlighted in
664 light blue and loops S51-F54 and V314-K318 in dark blue (Liu *et al.* 2014). Changes in
665 the main chain course for yeast SQS are shown in red; non conserved residues of N113-
666 D119 and D161-T171 fragments are shown as sticks.

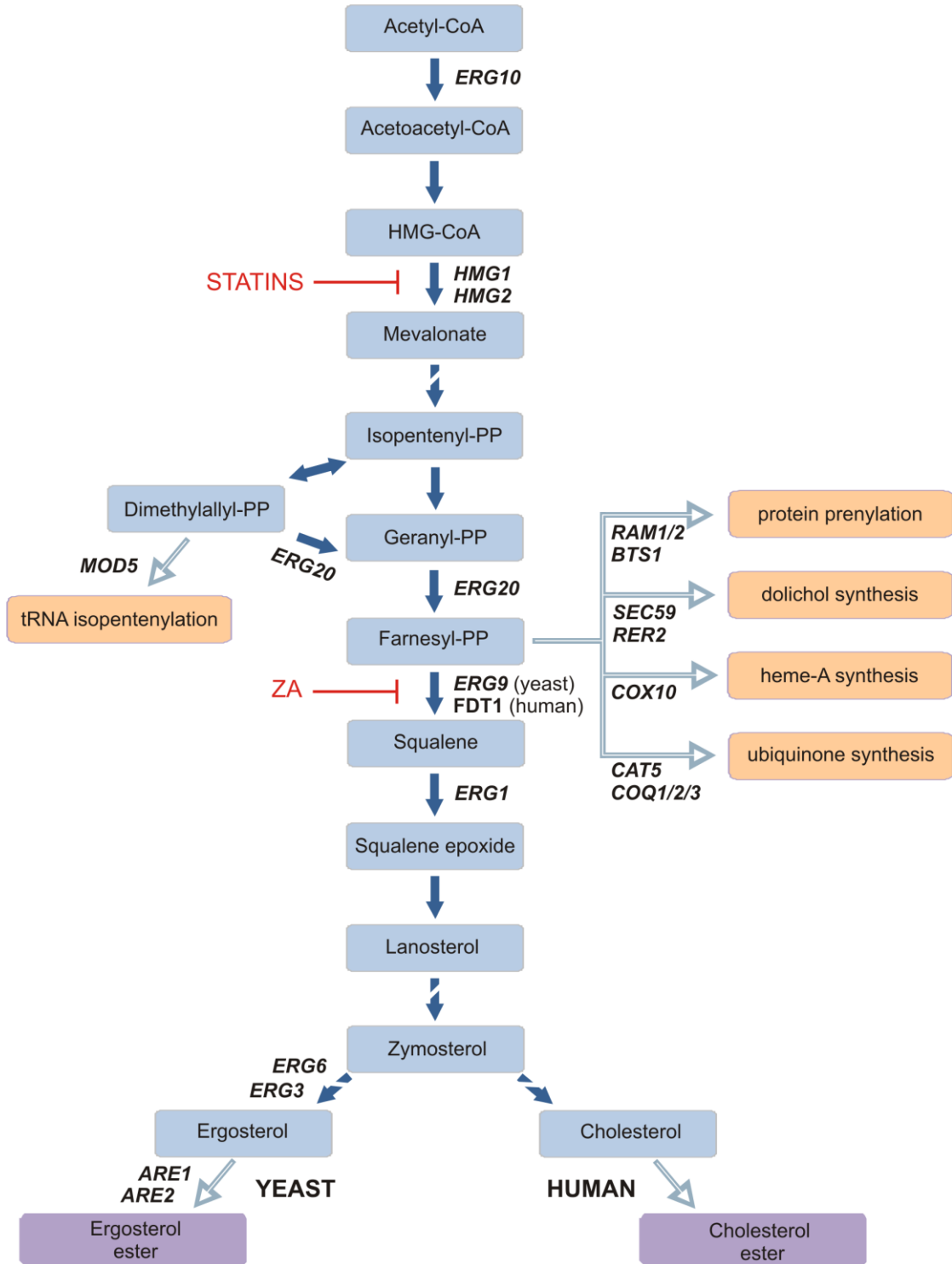
667 **Figure S3** Alignment of yeast (Y) and human (H) SQS amino acid sequences. The
668 hybrid human-yeast SQS protein consists of amino acid residues 1-296 of human SQS
669 and residues 304-444 of yeast SQS. Arrow indicates the exchanged regions. Stars
670 indicate identical amino acid residues. Sequences were aligned using the COBALT
671 server (Papadopoulos and Agarwala 2007).

672 **Figure S4** The steady-state squalene synthase protein (SQS-HA) level in the *erg9Δ*
673 [$P_{ERG9-HYBHA}$] strain.

674

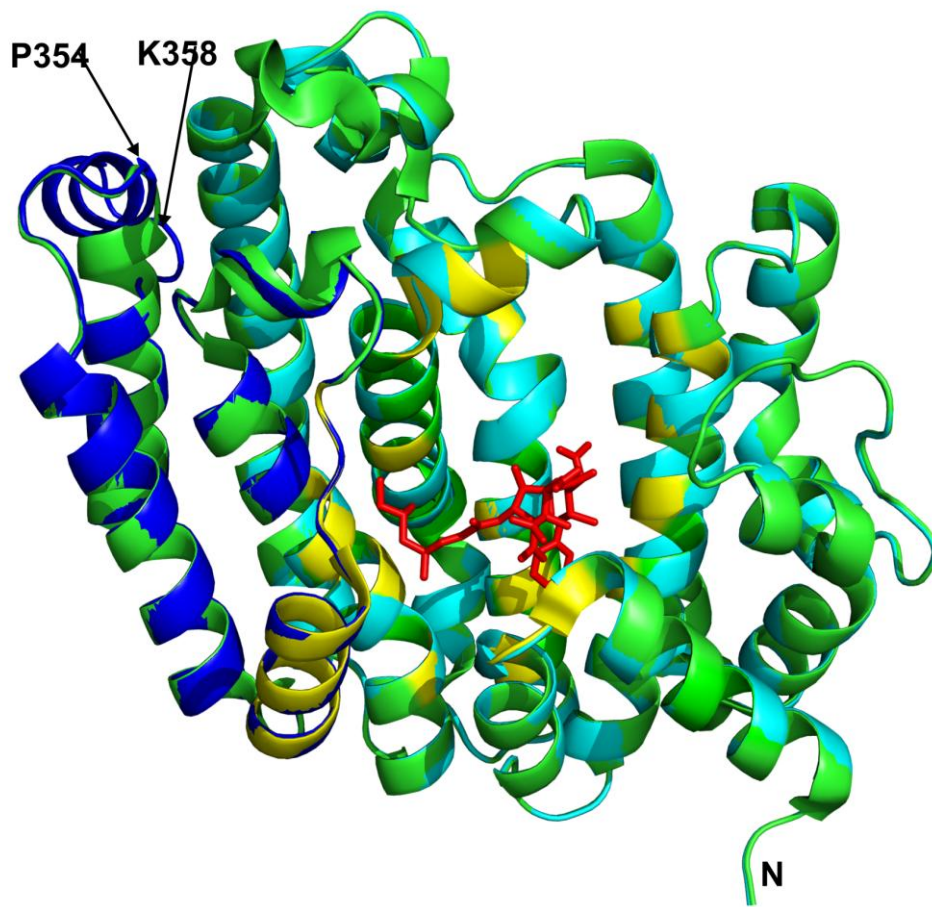
675

676



677

678



679

680

681

682

683

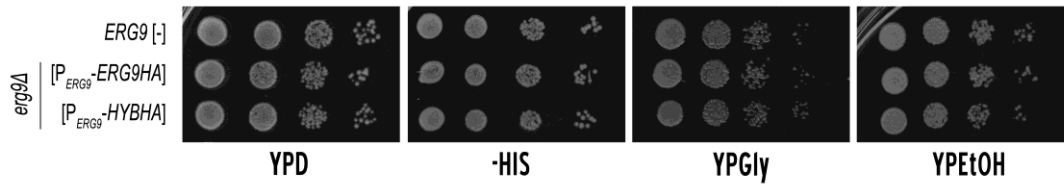
684

685

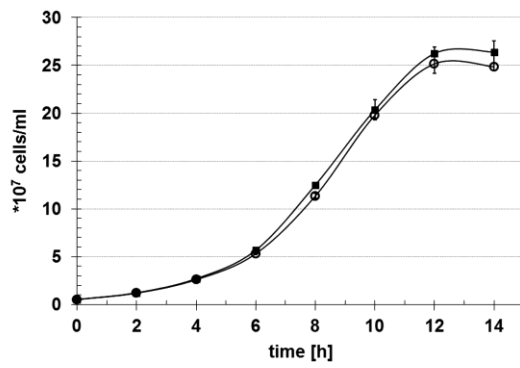
686

687

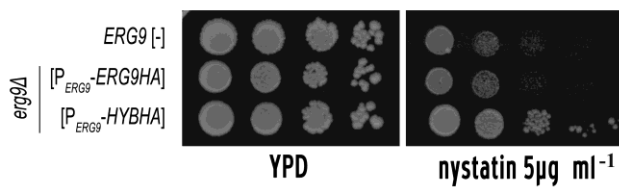
(a)



(b)



(c)



688

689

690

691

692

693

694

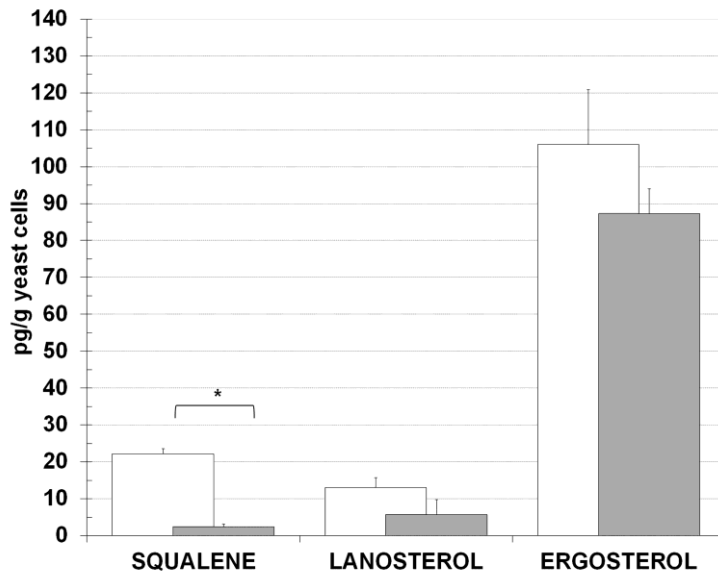
695

696

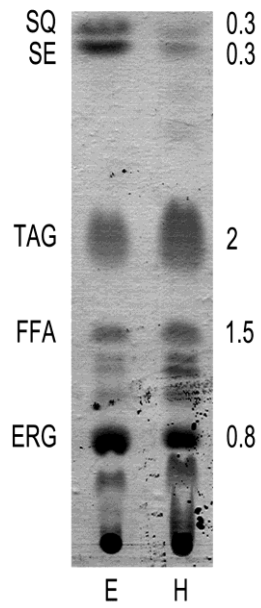
697

698

(a)



(b)



699

700

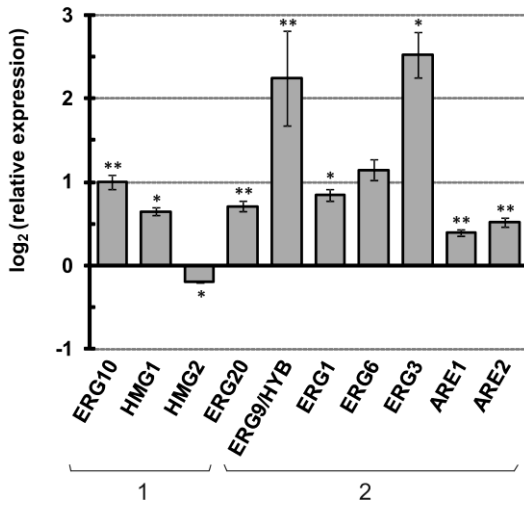
701

702

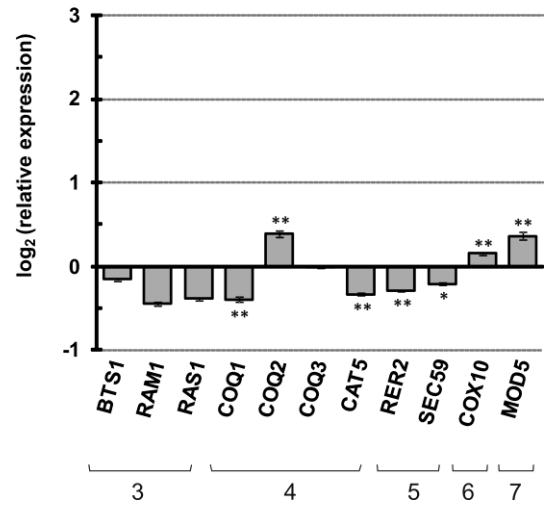
703

704

(a)

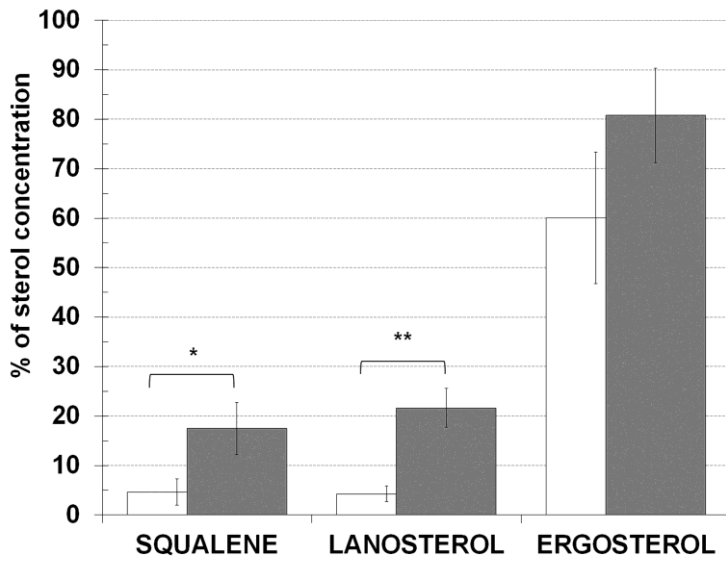


(b)



705

706



707

708

709

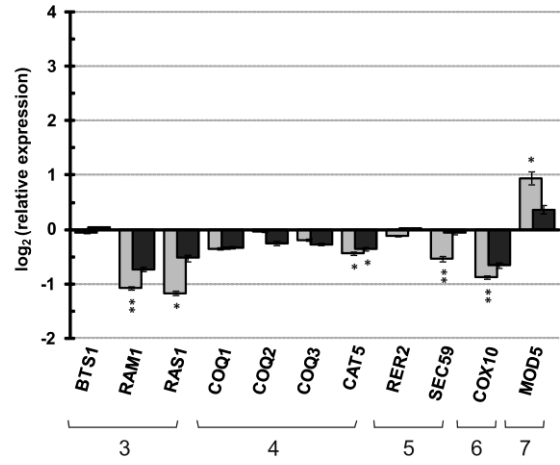
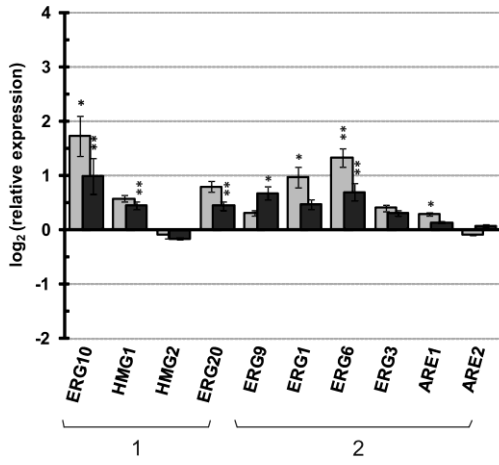
710

711

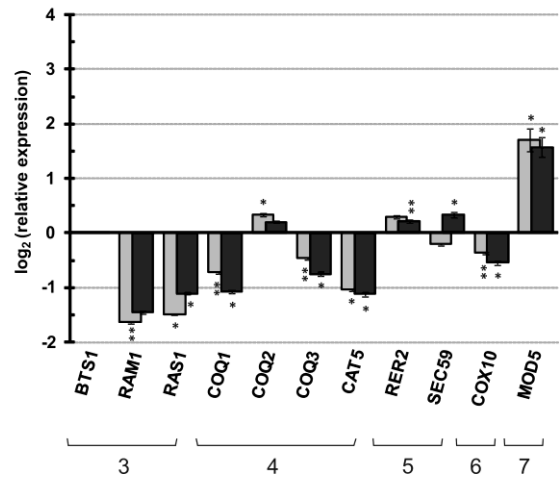
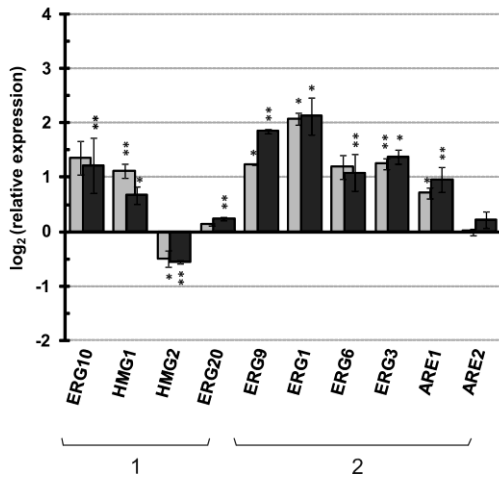
712

713

(a)



(b)



714